A Study of the Drawing Behavior of Poly(ethylene Terephthalate)

J. M. PERENA,* R. A. DUCKETT, and I. M. WARD, *Department of Physics, University of Leeds, Leeds LS2 9JT, United Kingdom*

Synopsis

Cold-drawn and hot-drawn samples of poly(ethylene terephthalate) were studied by means of measurements of shrinkage stress, birefringence, and differential scanning calorimetry (DSC). The values of shrinkage stress were comparable for both types of sample, implying that the deformation of a molecular network is important for both cold drawing and hot drawing. The DSC results indicate that substantial crystallization occurs in hot drawing for other than the lowest draw ratios, and this crystallization gives rise to an additional peak in the shrinkage stress measurements. In addition to temperature, strain rate is also an important variable, and changes in strain rate caused significant changes in both hot-drawn and cold-drawn samples.

INTRODUCTION

In a previous investigation[1] the drawing behavior of poly(ethylene terephthalate) (PET) was studied over the temperature range of 20–80°C. Birefringence measurements on the drawn materials were combined with shrinkage stress data in an attempt to understand the change in the drawing behavior from cold drawing through a neck in the range of 20–60°C to homogeneous drawing at temperatures above the glass transition. It was found instructive to examine the results of these studies within the framework of homogeneous deformation mechanisms, especially in terms of the deformation of a molecular network. In this paper, we describe comparable studies on cold-drawn and hot-drawn PET, particularly addressing the question as to when the possible onset of crystallization occurs—either during the drawing processes or during the shrinkage stress measurements—which continue to be valuable as a diagnostic tool for the analysis of possible deformation mechanisms.

EXPERIMENTAL

Drawing Procedures

In all cases the initial material was an isotropic PET film of 145 μm thickness. Specimens for drawing were prepared by carefully cutting 4-mm-wide strips with a scalpel, holding the sheet on graph paper to ensure parallelity. The number-average molecular weight of the film was estimated to be 1.8×10^4, on the basis of an intrinsic viscosity determination on a 1% solution in *o*-chlorophenol at 28.0°C and the previously established[2] relationship $\eta = 1.7 \times 10^{-4} M_n^{0.83}$.

The specimens were uniaxially drawn in an Instron tensile testing machine, either in a conditioning chamber at 80°C to obtain homogeneous hot drawing

* Present address: Instituto de Plasticos Y Caucho, Juan de la Cierva, 3, Madrid-6, Spain.

Journal of Applied Polymer Science, Vol. 25, 1381–1390 (1980)

0021-8995/80/0025-1381$01.00

or at room temperature (20°C) to study the cold-drawing process. The crosshead speeds ranged from 0.1 to 20 cm/min, and the calculated nominal strain rates are based on the initial specimen lengths.

Hot-drawn specimens were produced at nominal draw ratios of 1.3, 1.5, 1.7, 2, 2.5, 3, 4, 4.5, and 4.8. For cold drawing, both isotropic specimens and preoriented specimens prepared by hot drawing were used, and these were then drawn to their natural draw ratios. In all cases the actual draw ratios were determined from the displacement of ink marks in the homogeneous drawn portion of the final specimen, which were initially spaced at intervals of 2 mm.

Optical Measurements

Refractive indices were measured using a Zeiss (Jena) Interphako image-splitting interference microscope, the samples being embedded in accurately calibrated immersion liquids. All the measurements were carried out at 551 nm and the results corrected for any deviations of temperature from 20°C.

A quicker characterization of the sample could be obtained by measuring the birefringence of the samples with an Ehringhaus compensator. This method suffers from the difficulty of identifying the zero-order fringe because of the different dispersion characteristics of PET and calcite. Cross-calibration of the two methods showed a systematic error in the compensator method, so all compensator results were corrected to allow for this using a master calibration graph.

Differential Scanning Calorimetry (DSC)

A Perkin–Elmer differential scanning calorimeter DSC II was used for the thermal measurements, all of which were undertaken at a standard heating rate of 10°C/min. Samples of ~5 mg were weighed with a Beckmann microbalance. The calorimeter was calibrated with indium, and the temperatures shown on the trace were corrected for hearing rate in the usual manner. Peak areas were measured with a planimeter.

Shrinkage Stress

The shrinkage stresses were determined in a specially constructed apparatus which is described in detail elsewhere.[3] The principle of the method[4] is to immerse the sample, which is in series with a nonbonded strain gauge transducer in a silicone oil bath at different temperatures (in this instance 80, 85, and 90°C). The shrinkage stress is then measured as a function of time by taking the transducer output to a chart recorder.

RESULTS AND DISCUSSION

Optical Measurements

For the hot-drawn samples, we followed the procedures outlined in previous publications.[5,6] First, to confirm that the samples were transversely isotropic, the refractive index of the isotropic polymer n_i was calculated from the relationship

$$\frac{n_i^2 - 1}{n_i^2 + 2} = \frac{1}{3}\frac{d_i}{d_0}\left[\frac{n_z^2 - 1}{n_z^2 + 2} + \frac{2(n_x^2 - 1)}{n_x^2 + 2}\right]$$

where d_i and d_0 are the density of isotropic undrawn and drawn samples, and n_z and n_x are the refractive indices along and perpendicular to the draw direction, respectively. The results are shown in Table I and confirm that this is a reasonable assumption.

Secondly, we can then proceed to calculate the optical molecular orientation average $[P_2(\theta)]_{opt}$ from the expression

$$\frac{\Delta\alpha}{3\alpha_0}[P_2(\theta)]_{opt} = \frac{\phi_z^e - \phi_x^e}{\phi_z^e + 2\phi_x^e}$$

where

$$\phi^e = \frac{n^2 - 1}{n^2 + 2}$$

and $\Delta\alpha/3\alpha_0 = 0.105$, as estimated from measurements on highly oriented samples. In Figure 1 the values of $[P_2(\theta)]_{opt}$ for the hot-drawn samples are shown as a function of $\lambda^2 - \lambda^{-1}$. It can be seen that, as observed previously, the results are consistent with the deformation of a network with N random links per chain where

$$[P_2(\theta)] = \frac{\lambda^2 - \lambda^{-1}}{5N}$$

The straight line of the figure indicates a correlation coefficient of 0.996 and values for N of 5.7, which is consistent with previous studies.[4,5]

A series of cold-drawn samples was prepared by drawing isotropic and hot-

TABLE I
Refractive Index Measurements

Draw ratio	Density (g/cm³)	n_z	n_x	n_i (predicted)	$[P_2(\theta)]_{opt}$
1	1.337	1.577	1.577	1.577	0
2.00	1.343	1.590	1.571	1.574	0.085
2.57	1.347	1.616	1.566	1.577	0.221
3.09	1.351	1.642	1.555	1.576	0.382
3.98	1.357	1.677	1.545	1.577	0.570

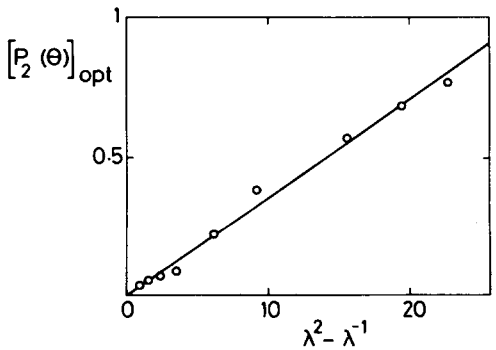

Fig. 1. $[P_2(\theta)]_{opt}$ as a function of $\lambda^2 - \lambda^{-1}$ for hot-drawn samples.

drawn samples with draw ratios less than 2. It was observed that the total draw ratio (i.e., product of the hot and cold draw ratios) was approximately 4, as observed previously.[7,8] Two draw rates were adopted for cold drawing. At the lower draw rate all the drawn samples were similar in appearance to hot-drawn samples. As previously proposed it was found that the *increase* in birefringence, $\Delta(\Delta n)$, related to the draw ratio in the cold-drawing stage according to the pseudoaffine deformation scheme[9,10] (Fig. 2). At the higher cross-head speed of 10 cm/min, isotropic samples displayed what has been termed "autovibrational stretching,"[11,12] the neck showing alternating transparent and silvery bands. The $[P_2(\theta)]_{opt}$ values for the high strain rate fall below the pseudoaffine curve, suggesting that the deformation begins to approach the network deformation scheme. A possible explanation is that there is a temperature rise at these strain rates as noted in previous work,[7] which, although not sufficient to raise the temperature above T_g, does permit more molecular mobility than that which occurs for isothermal deformation in the glassy state.

Shrinkage Stress Measurements

The shrinkage stress results for low draw ratios ($\lambda < 2$) are illustrated by the plots shown in Figure 3(a). It is to be noted that it takes 3 sec to reach the maximum shrinkage stress at 80°C compared with 0.6 sec at 89.1°C. However, the magnitude of the maximum shrinkage stress is similar for all temperatures. Similar data to those in Figure 3(a) are extended to longer times in Figure 3(b) to show that for low draw ratios, the shrinkage stress decays monotonically. For draw ratios higher than 2, a broad second peak occurs in the shrinkage stress curves at times ranging from 1 to 4 min. This second peak is more pronounced the higher the shrinkage temperature, and it broadens as the draw ratio is increased. A typical curve is shown in Figure 4. The DSC results in the next section are consistent with the view that this second peak is associated with

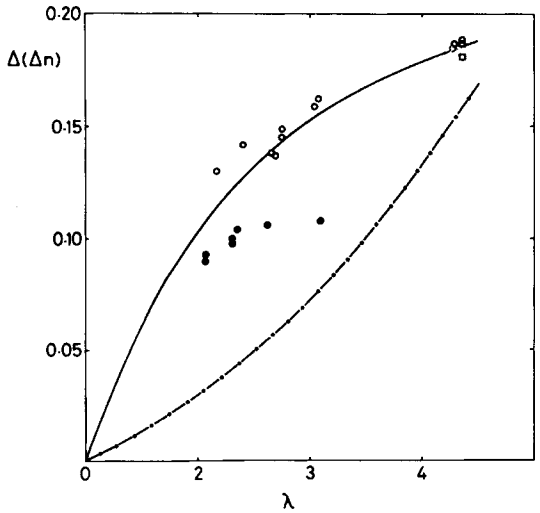

Fig. 2. Increase in birefringence $\Delta(\Delta n)$ as a function of draw ratio λ, for cold-drawn samples: (○) 0.2 cm/min; (●) 10 cm/min; (—) pseudoaffine deformation scheme with $\Delta n_{max} = 0.24$; (•—•) network model; $N = 5.7$ and $\Delta n_{max} = 0.24$.

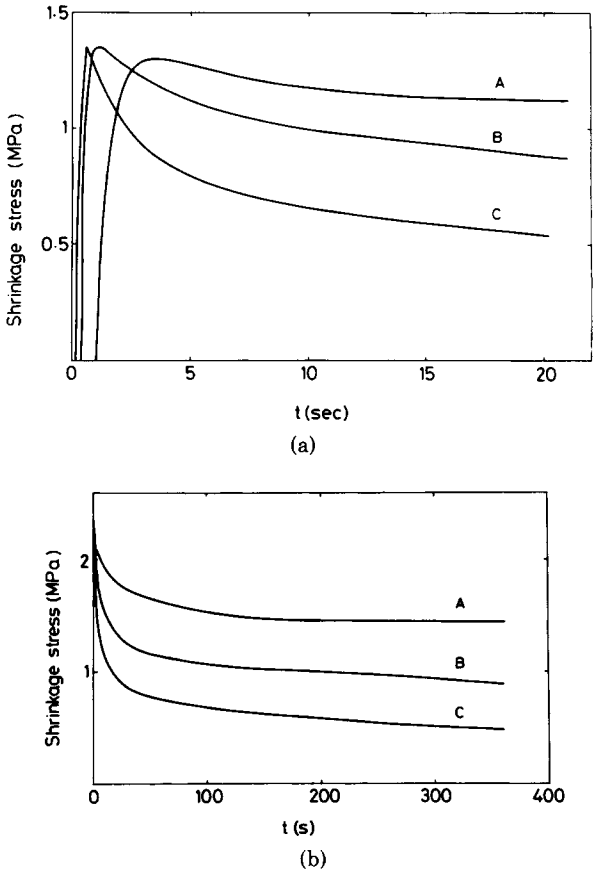

Fig. 3. (a) Shrinkage stress–time plots for $\lambda = 1.31$: A, 80°C, B, 84.7°C; C, 89.1°C. (b). Shrinkage stress–time plots for $\lambda = 2.57$: A, 80.1°C; B, 84.6°C; C, 88.9°C.

crystallization during the shrinkage experiment. We will also see that there is evidence from DSC measurements for crystallization during the actual drawing process for samples with $\lambda > 2$. Further confirmation of this was obtained from measurements of sample birefringence after the shrinkage stress measurement. Whereas the sample birefringence had decreased for $\lambda < 2.5$, at higher draw ratios, the birefringence was greater than before the shrinkage stress measurement and, remarkably, for heating times as short as 12 sec.

DSC Measurements

Isotropic PET Film

DSC measurements were undertaken on the isotropic PET film to establish the nature of possible changes taking place during the hot drawing process at 80°C. The thermograms of the isotropic film show three features. The first feature corresponds to the glass transition and appears at 71°C. The second feature is an exothermic crystallization peak at 143°C, and the third is the endothermic melting point at 251°C. The enthalpy changes associated with

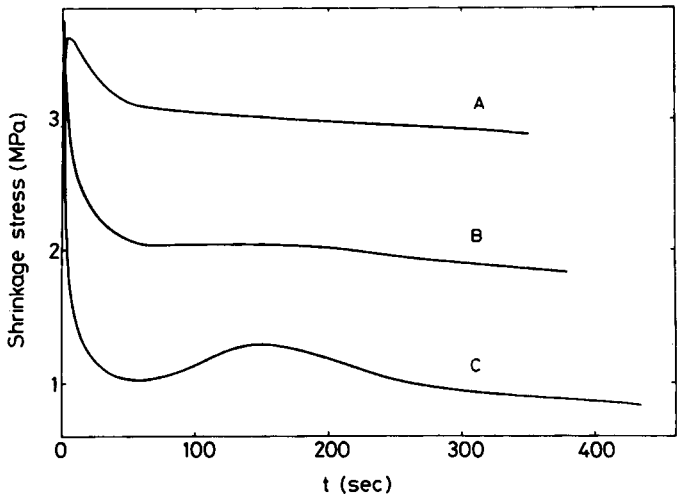

Fig. 4. Shrinkage stress–time plot for $\lambda = 2.57$: A, 80.1°C; B, 84.5°C; C = 89.1°C.

crystallization (ΔH_c) and melting (ΔH_m) were found to be 7.5 and 11.0 cal/g, respectively.

When the isotropic sheet was annealed at 80°C for 15 min (corresponding to the drawing conditions) the crystallization and melting peaks were unchanged but the temperature of the glass transition peak increased by 6 to 77°C. Similar effects were reported by previous workers,[13] who also claimed that further annealing at 78.5°C for 4 min reduced T_g to its initial value, in contrast to our results.

It is clear from these results that crystallization does not take place in the isotropic sheet at 80°C. The crystallization which occurs on drawing at 80°C must therefore take place during the drawing process itself.

It has been shown that annealing isotropic PET close to its melting point has a dramatic effect on the subsequent thermograms.[14–17] We have studied the effect of heat treatment at lower temperatures and have found that as the annealing temperature increases from 110 to 150°C and/or the annealing time increases from 0 to 50 min, both the glass transition peak and the crystallization peak diminish in intensity until they become undetectable for samples annealed at 150°C for 5 min. Moreover, in DSC traces of samples annealed at 140 and 150°C, a very small new endothermic peak developed 10°C above the heat treatment temperature. For example, we can see in Figure 5 how the samples annealed at 110°C show a steady decrease in both the crystallization temperature and the crystallization enthalpy as the annealing time increases. On the other hand, the melting temperature and ΔH_m did not change, and when it could be observed closely, a constant value of 77°C for T_g was found.

Hot-Drawn Samples

For hot-drawn samples, as the draw ratio increases in the range up to 2.5, the crystallization exotherm diminishes. For $\lambda > 2.5$, there is not a true peak but a drop on the DSC trace followed by an almost straight line up to the melting endotherm, making any quantitative analysis difficult. The results in Figure

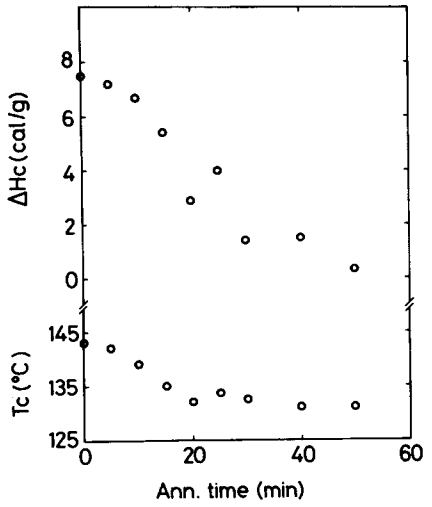

Fig. 5. Crystallization enthalpy ΔH_c and peak crystallization temperature T_c for isotropic PET as a function of annealing time for samples annealed at 110°C.

6 show how T_c falls by more than 40°C from isotropic sheet to $\lambda = 2.5$ and that the corresponding crystallization enthalpy also falls by almost a factor of 2. If we refer to the onset of the crystallization peak instead of the peak itself, it is possible to plot results for all drawn samples (bottom curve, Fig. 6).

These results suggest that the structural changes owing to molecular orientation affect the crystallization behavior even at the lowest draw ratios. Although it may still be valid to model the development of molecular orientation during

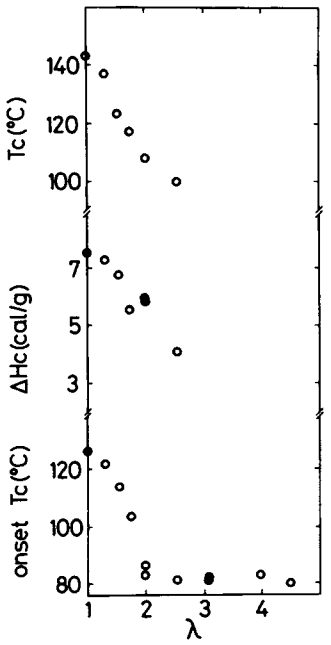

Fig. 6. Peak crystallization temperature T_c, crystallization enthalpy ΔH_c, and onset of crystallization temperature for hot-drawn samples as a function of λ.

hot drawing by the stretching of a rubber network on the grounds that crystallization occurs subsequent to molecular orientation, the interpretation of shrinkage force measurements is clearly much less secure, especially for $\lambda > 2.5$.

Annealed Drawn Samples

With a view to understanding the nature of the shrinkage stress measurements, we also undertook DSC measurements on hot-drawn samples annealed at 87°C for 1, 2, 3, and 4 min. As can be seen from Figure 7(a), the peak crystallization temperature falls with draw ratio. At higher draw ratios the crystallization peak cannot be discerned, as already discussed. The results in Figure 7(b) show that there is also a considerable decrease in the crystallization enthalpy with increasing draw ratio and, at the higher draw ratios, with annealing time. These results do confirm that for draw ratios of $\lambda > 2$, the onset of crystallization occurs above 80°C, i.e., above the drawing temperature. It is also clear from the results shown in Figure 6 that the onset of crystallization for $\lambda > 2$ falls within the range of the 87°C shrinkage stress temperature. All these results are consistent with the presence of a second peak in the shrinkage stress measurements only for temperatures ~90°C and draw ratios higher than 2.

Shrinkage Stress–Birefringence Correlations

It was shown[4] that for the low degrees of molecular orientation produced in PET fiber spinning processes (birefringence < 0.012) the shrinkage force is linearly related to the birefringence, i.e., there is a constant stress optical coefficient corresponding to approximately three monomers per random link. Our more recent work has shown[1] that this correlation also holds for hot-drawn PET but only at low draw ratios. This conclusion is confirmed by the present results for hot-drawn samples, shown in Figure 8. At higher draw ratios (corresponding to $\Delta n > 0.02$) the simple linear relationship no longer holds. Moreover, there are distinct differences between samples drawn at different rates. These dif-

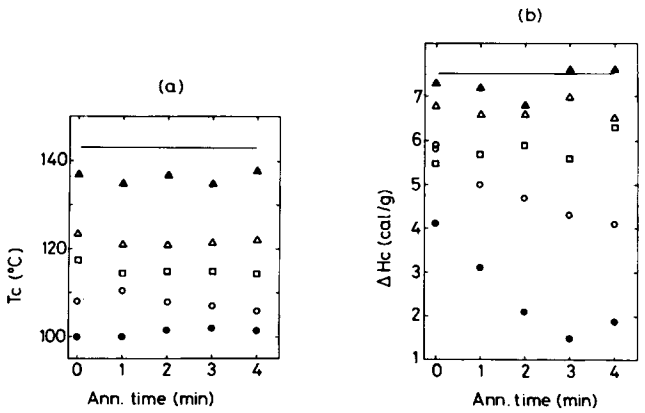

Fig. 7. (a) Peak crystallization temperature T_c. (b) Crystallization enthalpy ΔH_c as a function of annealing time at 87°C for various draw ratios: (▲) 1.3; (△) 1.53; (□) 1.73; (○) 2.0; (●) 2.57.

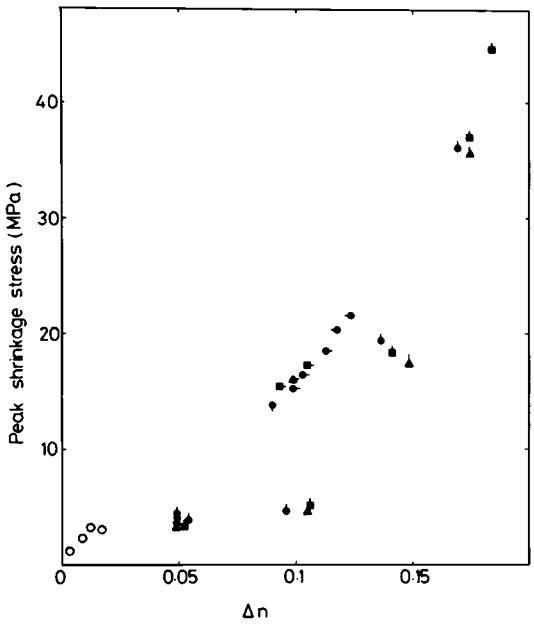

Fig. 8. Peak shrinkage stress as a function of birefringence. Shrinkage temperature 90°C. (●) 3.3×10^{-2}; (—●) 1.3×10^{-3}; (●—) 6.4×10^{-4}; (●) 3.2×10^{-4}. Shrinkage temperature 85°C: (■) 3.3×10^{-2}; (—■) 1.3×10^{-3}; (■—) 6.4×10^{-4}; (■) 3.2×10^{-4}; Shrinkage temperature 80°C: (▲) 3.3×10^{-2}; (—▲) 1.3×10^{-3}; (▲—) 6.4×10^{-4}; (▲) 3.2×10^{-4}.

ferences could arise from either differences in molecular orientation or crystallization, or possibly both. The DSC results suggest that careful studies of the onset of crystallization will be required before a satisfactory explanation of the shrinkage stress data can be advanced.

The corresponding results for the cold-drawn samples are shown in Figure 9, where the peak shrinkage stress is plotted as a function of total birefringence

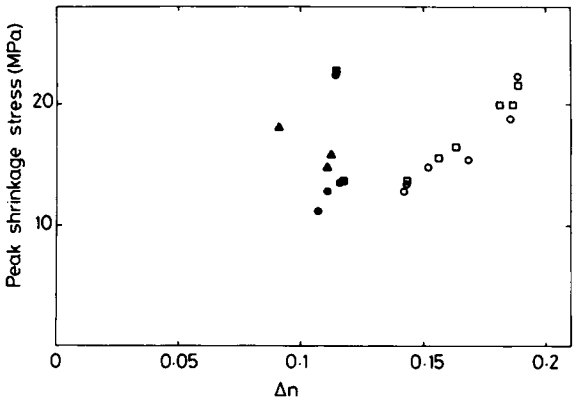

Fig. 9. Peak shrinkage stress as a function of total birefringence Δn: (○ ●) shrinkage temperature 90°C; (□ ■) 85°C; (△ ▲) 80°C. Open points: cross-head speed 0.2 cm/min; filled points: 1.0 cm/min.

Δn. [Because the birefringence introduced at the hot-drawing stage is comparatively small, a very similar plot is produced by plotting as a function of $\Delta(\Delta n)$]. It is interesting to note that the shrinkage stresses are comparable in magnitude to those of the hot-drawn samples, which implies that the deformation of a molecular network is also important for cold drawing. These preliminary results suggest that strain rate effects are again also important but of a different form to those seen in hot drawing. Further work is required to elucidate the origin of these differences.

We wish to acknowledge the financial support given to one of the authors (J.M.P.) by the Ramsay Memorial Fellowship Trust during the period when this research was undertaken.

References

1. F. Rietsch, R. A. Duckett, and I. M. Ward, *Polymer,* **20,** 1133 (1979).
2. D. A. S. Ravens and I. M. Ward, *Trans. Faraday Soc.,* **57,** 150 (1961).
3. G. Capaccio, T. A. Crompton, and I. M. Ward, to be published.
4. P. R. Pinnock and I. M. Ward, *Trans. Faraday Soc.* **62,** 1308 (1966).
5. A. Cunningham, I. M. Ward, H. A. Willis, and V. I. Zichy, *Polymer,* **15,** 749 (1974).
6. M. Kashiwagi, A. Cunningham, A. J. Manuel, and I. M. Ward, *Polymer,* **14,** 111 (1973).
7. S. W. Allison and I. M. Ward, *Br. J. Appl. Phys.* **18,** 1151 (1967).
8. J. S. Foot and I. M. Ward, *J. Mater. Sci.,* **10,** 955 (1975).
9. I. M. Ward, *Mechanical Properties of Solid Polymers,* Wiley, London, 1971, p. 258.
10. I. M. Ward, *Br. J. Appl. Phys.,* **18,** 1165 (1967).
11. A. S. Kechek'ayn, G. P. Adrianova, and V. A. Kargin, *Polym. Sci. USSR,* **12,** 2743 (1970).
12. R. Rosen, *J. Mater. Sci.,* **9,** 929, (1974).
13. E. Ito, K. Yamamoto, Y. Kobayashi, and T. Hatakeyama, *Polymer,* **19,** 39 (1978).
14. M. Droscher and G. Wegner, *Polymer,* **19,** 43 (1978).
15. S. Fakirov, E. W. Fischer, R. Hoffmann, and G. F. Schmidt, *Polymer,* **18,** 1121 (1977).
16. R. C. Roberts, *Polymer,* **10,** 117 (1969).
17. P. J. Holdsworth and A. Turner-Jones, *Polymer,* **12,** 195 (1971).

Received October 10, 1979